DOI: 10.31401/WS.2020.proc.25

The GIC growth in electric power lines during magnetic storm on 7-8 September 2017

Belakhovsky V.B.[1], Pilipenko V.A.[2], Sakharov Ya.A.[1], Selivanov V.N.[3]

[1]Polar Geophysical Institute, Apatity
[2]Institute of the Physics of the Earth, Moscow
[3]Kola Scientific Center RAS, Apatity

Abstract. It is considered the growth of the geomagnetically induced currents (GIC) in electric power lines at Kola Peninsula and Karelia (Russia) during strong geomagnetic storm 7-8 September 2017. We used the GIC registration system in electric power lines created by the Polar Geophysical Institute and Kola Scientific Center. The IMAGE magnetometer data was used for the analyses of the geomagnetic field variability. The dY/dt has comparable contribution to the GIC growth as dX/dt. So these GIC are dangerous for the north-south oriented technological systems. There are two intervals of the strong GIC growth (more than 50 A) was registered during the storm. It is found that one interval the significant contribution have the vortex-like ionosphere current systems, for the another time interval auroral electrojet have dominant contribution in comparison with vortex current systems. The fine structure of the substorm (Pi3 pulsations) produce vortex-like current systems connected with the field-aligned currents in the magnetosphere.

1. Introduction

One of the most significant factors of space weather for terrestrial technological systems is geomagnetically induced currents (GICs) in conductor systems caused by abrupt changes of the geomagnetic field [*Lanzerotti*, 2001]. GICs associated with great magnetic disturbances were found to be dangerous for various technological systems, causing malfunction of railway equipment, disruption of ground and transatlantic communication cables, deleterious impacts on telephone lines, and reduction of the lifetime of pipelines [*Pirjola et al.* 2005].

GIC are often modeled as fluctuations of intensity of the East-West auroral electrojet producing telluric currents in the longitudinal direction [*Boteler et al.* 1998]. On the basis of these notions, it is commonly supposed that geomagnetic disturbances are most dangerous for technological systems (like power lines, and oil/gas pipe lines) extended in the longitudinal direction. However, it was found that fast small-scale ionospheric current structures can provide a significant contribution to rapid geomagnetic field variations, responsible for GIC generation [*Viljanen et al.* 2001; *Belakhovsky et al., 2018; Belakhovsky et al., 2017*]. Thus, to characterize the geomagnetic field variability one needs finer characteristics than the widely used time derivative of the *X*-component (North-South) of the geomagnetic field d*X*/dt [*Belakhovsky et al., 2019*]. It is still tempting to find an adequate tool to reveal the temporal-spatial features of geomagnetic field variations most relevant to the GIC generation.

[Dimmock et al., 2019] examined the impact of this storm on GIC in a gas pipeline in southern Finland. Although this storm was moderate as judged by the global Dst index (~ - 150 nT), it led to an unexpectedly large GIC burst (> 10 A), which had not previously been observed in this system even under large geomagnetic disturbances.

Here we consider the contribution of geomagnetic disturbances to the rapid growth of the GIC in electric power lines of Kola Peninsula and Karelia for the 7-8 September 2017 strong geomagnetic storm.

2. Data and methods

A system to monitor the impact of GIC on power lines was deployed in 2011 in the Kola Peninsula and Karelia by the Polar Geophysical Institute and the Center for Physical and Technical Problems of North's Energetic. The system consists of 4 stations at 330 kV power line and a station at the 110 kV power line. Each station records a quasi-DC current in the dead-grounded neutral of the transformer.

The variations of the geomagnetic field were measured by IMAGE magnetometers with 10-sec time resolution. For an array of magnetometers oriented along a geomagnetic meridian, the vector diagram method can be applied. The Finnish Meteorological Institute provides the online (http://space.fmi.fi/image/beta/) capability to compute and visualize 2D ionospheric equivalent current vectors from the IMAGE magnetometers. For the equivalent current modeling, the method of spherical elementary current systems has been used [*Amm & Viljanen*, 1999]. The technique determines the divergence-free component of the equivalent ionospheric currents (which roughly describes the distribution of ionospheric Hall currents) from ground-based magnetometer data.

3. GIC growth during magnetic storm on 7-8 September 2017

We consider the strong magnetic storm on 7-8 September 2017 that was initiated by an interplanetary shock arrival at ~23:30 UT on 7 September. After ~20:00 UT on 7 September, IMF Bz gradually turned southward (<0) and remained steady at about -10 nT to -30 nT until ~04:00 UT on 8 September. The solar wind speed reach the high value 870 km/s. This produced driving of the magnetosphere into a magnetic storm, during which geomagnetic indices reached maximal values of |Dst| ~150 nT and AE~2700 nT.

This period coincided with a period of maximum of magnetic bay magnitude at the IMAGE magnetic stations from 20-04 UT (Fig. 1). The magnetic bay was observed only in the *X*-component (more than 3000 nT at SOD station).

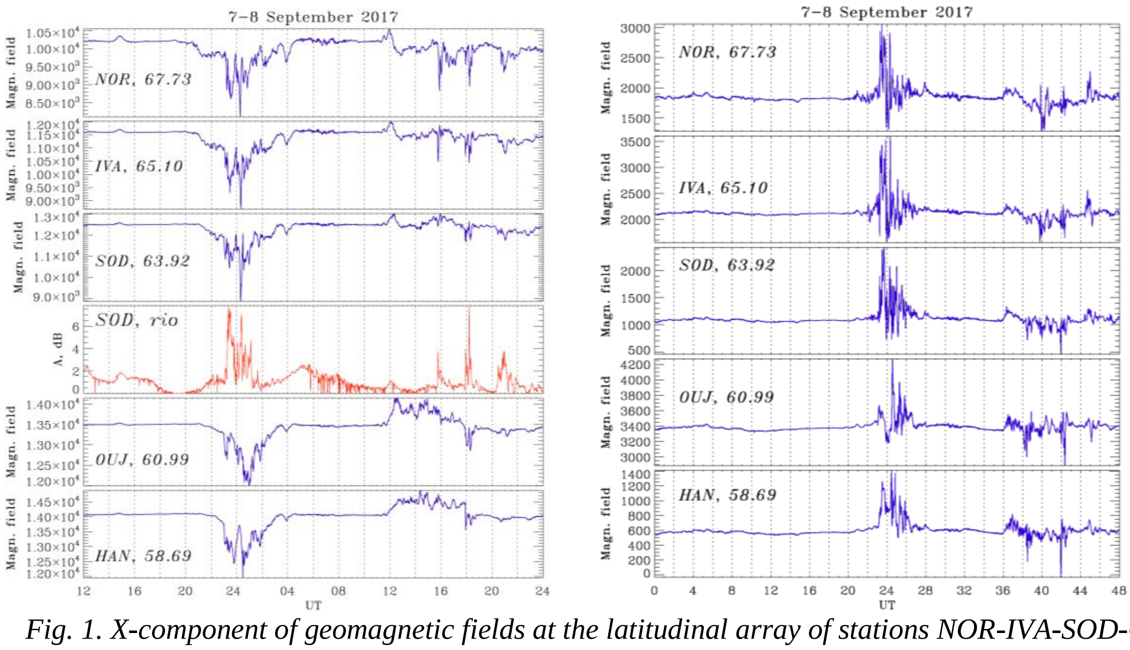

Fig. 1. X-component of geomagnetic fields at the latitudinal array of stations NOR-IVA-SOD-OUJ-HAN and the cosmic noise absorption at SOD riometer station [dB] (left panel), the Y-component of the geomagnetic field(right panel) for the 7-8 September 2017. Geomagnetic latitudes are indicated near the station codes.

During the period of maximal magnetic disturbance, intense Pi3 pulsations were superposed on the magnetic bay. These pulsations are not quasi-sinusoidal waves like typical Pc5 pulsations; they are rather quasi-periodic sequences of magnetic impulses. The time scale of these oscillations varies from ~20 min at lower latitudes up to ~10 min at higher latitudes (Fig. 1).

There are two peaks of the significant GIC growth (more than 50 A) was observed during this magnetic storm. During first interval extremely high values of GIC were recorded (up to ~85 A per node) at station VKH, from ~22:00 to ~02:00 UT on 7-8 Sept 2013 (Fig. 2). At lower latitude KND station the value of the GIC was about 15 A. The data for another GIC stations was not available for this event. The second peak of GIC was observed at 20 UT on 8 September 2017, it was short time increase (5-10 minutes).

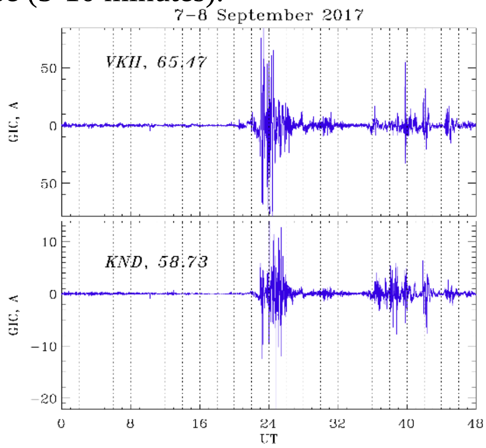

Fig. 2. GIC data at stations VKH, KND for the 7-8 September 2017. Geomagnetic coordinates are shown near station codes.

The substorm at 23-02 UT was accompanied by the strong increase of the cosmic noise absorption (CNA) with amplitude more than 7 dB as seen from the SOD riometer, the second disturbance was accompanied by the growth of the CNA (>7 dB) as well. It testifies about the presence of the powerful electron precipitations into the ionosphere.

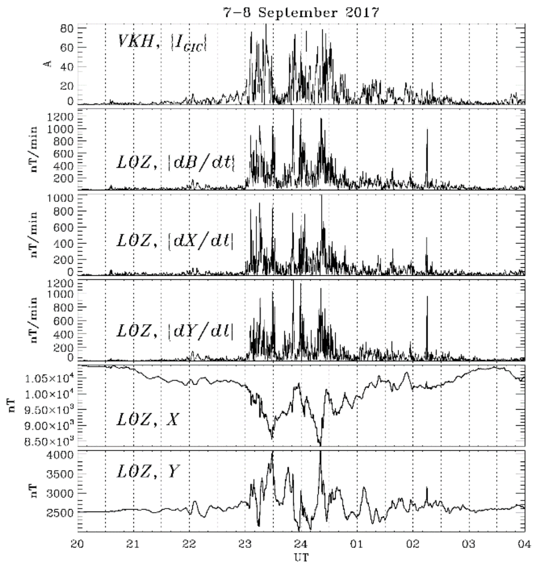

Fig. 3. Comparison between GIC amplitudes, time derivatives |dX/dt| and |dY/dt| [nT/min], and ΔX and ΔY components of geomagnetic field [10^4·nT] at nearby stations VKH and LOZ for the 7-8 September 2017.

During the magnetic storm the magnetic disturbance gradually increased and then slowly decayed, and was mainly oriented in the X-direction. However, during the maximal disturbance magnetic variations became more chaotic. Comparison of the magnitude of magnetic disturbances ΔX and ΔY with amplitudes of time derivatives |d*X*/dt|, |d*Y*/dt| (Fig. 3.) shows that though the magnetic disturbance was much larger in the X-component than in the Y-component, $|\Delta X|>>|\Delta Y|$, the time derivative $|dY/dt|\geq 1200$ nT/min was larger than the time derivative $|dX/dt|\geq 1000$ nT/min. Therefore, variations of both horizontal components provided a similar contribution to the increase of $|d\mathbf{B}/dt|$. Magnetic field variations are composed from time variations and variations caused by fast azimuthal drift of Pi3 structures.

To present the picture of the dynamics of ionospheric currents along the meridional profile, geomagnetic disturbances B = {X, Y} for each station of the profile were drawn on one graph in the form of sequentially time-shifted disturbance vectors. The perturbation of the magnetic field B at the observation point is associated with the equivalent ionospheric current J above it as follows $B = (2\pi/c)\ [J\times n]$, where n is the normal to the plane. Vector J is rotated by $\pi/2$ clockwise with respect to B (but its value will be indicated in nT).

The vector diagrams of the equivalent ionospheric current variations (Fig. 4.) with time cadence 1 min show that the Pi3 pulsations were a sequence of localized vortex-like structures for the interval 15-22 UT. But for the interval 20-04 UT it is seen the dominant contribution of the auroral electrojet.

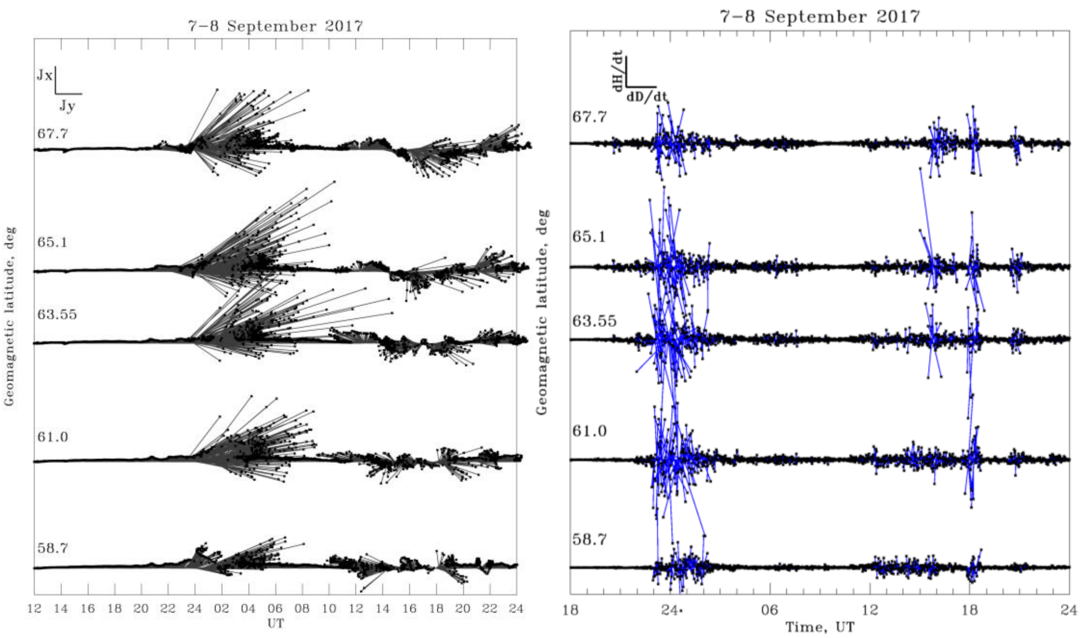

Fig. 4. Vector diagrams of equivalent ionosphere currents (left panel) and the vector diagram of the dB/dt (right panel) for the 7-8 September 2017 with time cadence 1 min.

The spherical elementary current method (SECS) [Amm and Viljanen, 1999] is used to calculate the field of equivalent currents. The method is based on the division of horizontal currents integrated over the height of the ionosphere into vortex (divergence-free) and potential components. Horizontal irregular currents close the field-aligned currents connecting the upper atmosphere with magnetospheric processes. From the ground data, a divergence-free (vortex) component is calculated, which approximately describes the distribution of the ionospheric Hall currents. These method of 2D equivalent currents reveals the formation of the vortex-like intensifications during the growth of GIC with epicenter at 66°-67° geomagnetic latitudes, i.e. under the Kola Peninsula (Fig. 5.). It is seen that for some moments the ionosphere currents have vortex-like structure (left panel), for another moment the structure of the ionosphere currents is complicate. It seems like a mixture of the auroral electrojet and vortex like currents connected with the field-aligned currents in the magnetosphere.

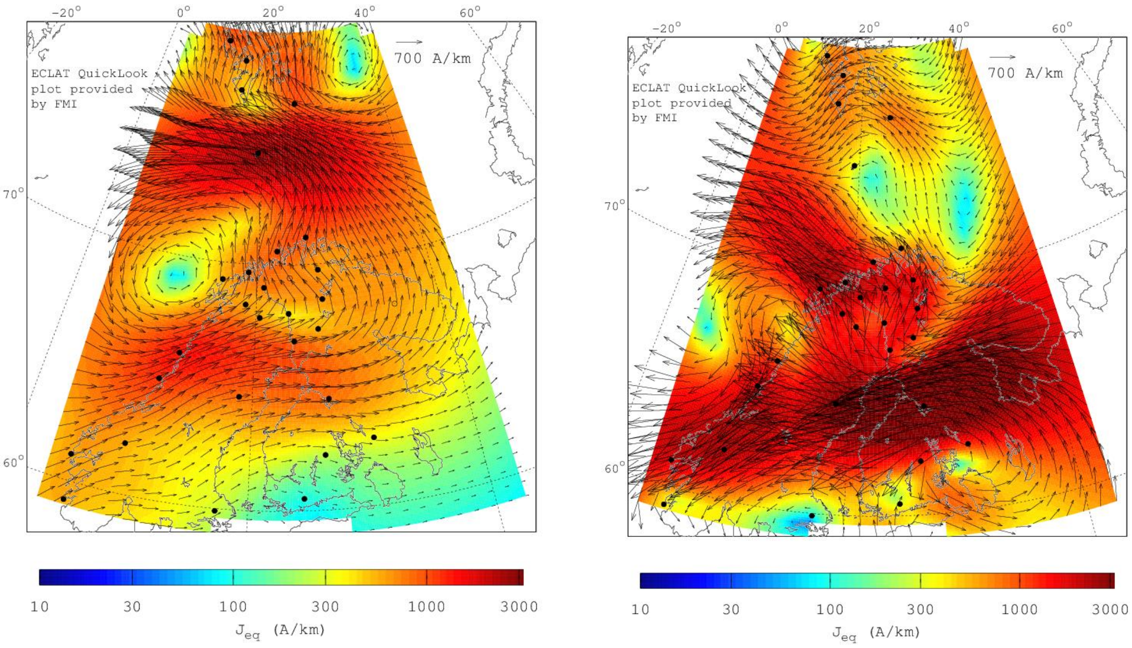

Fig. 5. The 2D model of equivalent ionosphere currents constructed from the IMAGE magnetometer data for the 7-8 September 2017 at 16.05 UT (left) and 23.57 UT (right).

A comparison of the instantaneous amplitudes of the GIC at VKH and KND stations with the "magnetic keogram", showing the time variation of the latitudinal distribution along the profile of the IMAGE stations of the amplitude of the geomagnetic disturbance (X-component) and the field variability dX / dt, is presented in Fig. 6. Six activations are accompanied by a burst of dB / dt and GIC. Disturbances of the magnetic field occur at latitudes 58°-67°. For all activations, a general tendency is visible - the disturbance first arises at high latitudes, and then spreads to lower ones.

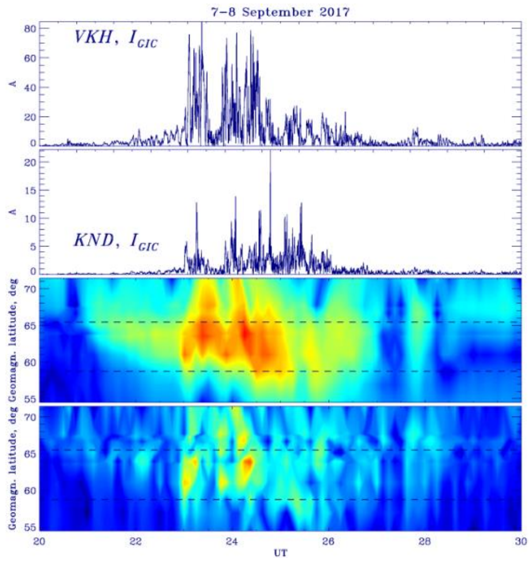

Fig. 6. The GIC at VKH, KND stations; latitude-UT distribution of the geomagnetic field variations (X-component) according to the IMAGE magnetometer data; latitude-UT distribution of the dX/dt.

The epicenter of the field variability dX/dt localized in latitude in the range of 60°-65°. The transmission lines from VKH to KND cover an overlapping area of latitudes, from 62° to 68°. Thus, during this magnetic storm, the "epicenter" of the geomagnetic disturbance was within the area covered by the power transmission line. The analysis of the spatial-temporal distribution of the geomagnetic field variations are does not coincide with the spatial-temporal distribution of its derivation during the strong GIC growth at VKH and KND stations. So the strong GIC is not always associated with the strong geomagnetic disturbance but it associated with fast geomagnetic disturbances embedded into strong magnetic bay.

4. Conclusions

The analysis of the geomagnetic disturbances and GIC variations for the strong magnetic storm 7-8 September 2017 shows that the large-scale structure of the X-component of the disturbed geomagnetic field is mainly determined by the ionospheric East-West electrojet. In smaller regional scales, weaker but rapidly varying localized vortex-like current systems are superposed on the electrojet. These current structures produce intense GICs, as observed by the GIC recording system of the power lines in the Kola Peninsula.

A quasi-periodic sequence of localized vortex-like structures observed by magnetometers produces very high values of GIC (up to ~85 A).The night-side solitary vortices observed as magnetic pulses with large amplitudes superposed on the substorm-related magnetic bay have been observed to be accompanied by very intense GICs. These results have confirmed that GIC cannot be modeled by a simple model of the extended ionospheric current and dictate the necessity to take into account superposed localized vortex-like current systems.

Reference

Amm O., A. Viljanen. Ionospheric disturbance magnetic field continuation from the ground to the ionosphere using spherical elementary current systems // Earth Planets Space, 51, 431-440, 1999.

Belakhovsky V.B., V.A. Pilipenko, Ya.A. Sakharov, D.L. Lorentzen, S.N. Samsonov. Geomagnetic and ionospheric response to the interplanetary shock on January 24, 2012 // Earth, Planets and Space, 69:105, doi:10.1186/s40623-017-0696-1, 2017.

Belakhovsky V.B., V.A. Pilipenko, Ya.A. Sakharov, V.N. Selivanov. Characteristics of the geomagnetic field variability for the study of the magnetic storm and substorm impact on electrical power systems // Physics of Solid State, №1, 173–185, 2018.

Belakhovsky V., Pilipenko V., Engebretson M., Sakharov Ya. and Selivanov V. Impulsive disturbances of the geomagnetic field as a cause of induced currents of electric power lines // Journal of Space Weather and Space Climate. 9. A18. 2019

Boteler D.H., R.J. Pirjola, H. Nevanlinna. The effects of geomagnetic disturbances on electrical systems at the Earth's surface // Adv. Space Res. 22, 17-27, 1998.

Dimmock A.P., Rosenqvist L., Hall J.-O., Viljanen A., Yordanova E., Honkonen I., André M., Sjöberg E.C. The GIC and geomagnetic response over Fennoscandia to the 7–8 September 2017 geomagnetic storm // *Space Weather*, *17*. 2019.

Lanzerotti L.J. Space weather effects on technologies // Space Weather, Geophys. Monogr. Ser. AGU. 125, p. 11, 2001.

Pirjola R., K. Kauristie, H. Lappalainen, A. Viljanen, A. Pulkkinen. Space weather risk // Space Weather. 3. S02A02. 2005.

Viljanen A., H. Nevanlinna, K. Pajunpaa, A. Pulkkinen. Time derivative of the geomagnetic field as an activity indicator. Ann. Geophys. 19. 1107-1118. 2001.

Acknowledgements. We thank the national institutes that support the IMAGE magnetic observatories (http://www.ava.fmi.fi/image). The interplanetary parameters were taken from the OMNI database (https://omniweb.gsfc.nasa.gov). We thank to the Sodankyla Geophysical Observatory (https://www.sgo.fi) for the possibility to use riometer data. Data from the PGI system are available at EURISGIC (European Risk for Geomagnetically Induced Currents) website http://eurisgic.org.